Korea-Australia Rheology Journal
Vol. 21, No. 1, March 2009 pp. 59-69

Numerical study on the effect of viscoelasticity on pressure drop and film thickness for a droplet flow in a confined microchannel

Changkwon Chung[1], Ju Min Kim[2], Kyung Hyun Ahn[1,*] and Seung Jong Lee[1]
[1]*School of Chemical and Biological Engineering, Seoul National University, Seoul 151-744, Korea*
[2]*Department of Chemical Engineering, Ajou University, Suwon 443-749, Korea*
(Received November 29, 2008; final revision received December 21, 2008)

Abstract

The prediction of pressure drop for a droplet flow in a confined microchannel is presented using FE-FTM (Finite Element - Front Tracking Method). A single droplet is passing through 5:1:5 contraction - straight narrow channel - expansion flow domain. The pressure drop is investigated especially when the droplet flows in the straight narrow channel. We explore the effects of droplet size, capillary number (Ca), viscosity ratio (χ) between droplet and medium, and fluid elasticity represented by the Oldroyd-B constitutive model on the excess pressure drop (Δp^+) against single phase flow. The tightly fitted droplets in the narrow channel are mainly considered in the range of $0.001 \le Ca \le 1$ and $0.01 \le \chi \le 100$. In Newtonian droplet/Newtonian medium, two characteristic features are observed. First, an approximate relation $\Delta p^+ \sim \chi$ is observed for $\chi \ge 1$. The excess pressure drop necessary for droplet flow is roughly proportional to χ. Second, Δp^+ seems inversely proportional to Ca, which is represented as $\Delta p^+ \sim Ca^m$ with negative m irrespective of χ. In addition, we observe that the film thickness (δ_f) between droplet interface and channel wall decreases with decreasing Ca, showing $\delta_f \sim Ca^n$ with positive n independent of χ. Consequently, the excess pressure drop (Δp^+) is strongly dependent on the film thickness (δ_f). The droplets larger than the channel width show enhancement of Δp^+, whereas the smaller droplets show no significant change in Δp^+. Also, the droplet deformation in the narrow channel is affected by the flow history of the contraction flow at the entrance region, but rather surprisingly Δp^+ is not affected by this flow history. Instead, Δp^+ is more dependent on δ_f irrespective of the droplet shape. As for the effect of fluid elasticity, an increase in δ_f induced by the normal stress difference in viscoelastic medium results in a drastic reduction of Δp^+.

Keywords : droplet microfluidics, pressure drop, film thickness, contraction and expansion flow, viscoelastic fluid, finite element method, front tracking method, Oldroyd-B model

1. Introduction

Droplet microfluidics has been rapidly developed since it has much potential for medical applications such as DNA assay (Griffiths and Tawfik, 2003; Sepp *et al.*, 2007; Tawfik and Griffiths, 1998), blood agglutination assay (Kline *et al.*, 2008), red blood cell hydrodynamics (Abkarian *et al.*, 2006), protein crystallization (Zheng *et al.*, 2004), and for chemical applications such as micro-reactors (Bringer *et al.*, 2004; Song *et al.*, 2003), transportation vessels (Abraham *et al.*, 2006; He *et al.*, 2005) and a release controller of encapsulated materials (Chu *et al.*, 2007). Droplets in microfluidic channels are usually transported by hydrodynamic force with the help of micropumps such as syringe pump or pneumatics. A proper micropumping should be conducted for reliable operation of the individual application (Laser and Santiago, 2004). However, pump design has been performed based on empirical knowledge since it is not straightforward to predict correct pressure drop in the complicated channel flows especially when the droplets or bubbles are involved.

Numerous works have focused on predicting the pressure drop and film thickness in terms of capillary number (Ca) which represents the relative effect of viscous force and interface tension. Fairbrother and Stubbs (1935) firstly conducted experimental works to find a relation for the film thickness (δ_f) $\sim Ca^{0.5}$ for $10^{-3} \le Ca \le 10^{-2}$. Taylor (1961) found the asymptotic limit of the film thickness to be approximately $2\delta_f/w \sim 0.55$ as Ca increases, which was later measured to be slightly larger (0.60) by Cox (1962). As a theoretical work, Bretherton (1961) derived a relation $\delta_f \sim Ca^{1/3}$ for very long bubbles in the limit of $Ca \to 0$. The pressure drop - velocity relation in the bubble flow was also investigated by Bretherton (1961). He reported that the pressure necessary to move a long bubble scales with

*Corresponding author: ahnnet@snu.ac.kr

$Ca^{-1/3}$ in the circular channel using the matched-asymptotic method which has been confirmed by succeeding studies (Edvinsson and Irandoust, 1996; Giavedoni and Saita, 1997; 1999; Heil, 2001; Kreutzer *et al.*, 2005; Ratulowski and Chang, 1989; Reinelt, 1987; Shen and Udell, 1985).

The relation between the film thickness and pressure drop was indirectly discussed with circular and polygonal channels in previous studies (Bretherton, 1961; Fairbrother and Stubbs, 1935; Wong *et al.*, 1995; 1995). The long bubble acts as a tight-fit piston in the circular channels, and as a result, the bubble and the fluid move roughly at the same speed (Bretherton, 1961; Fairbrother and Stubbs, 1935). On the other had in polygonal channels, the bubble acts as a leaky piston (Wong *et al.*, 1995; 1995), *i.e.*, the pressure work is dissipated predominantly by the corner flow between the bubble interface and the sidewalls. The estimated film thickness was proportional to $Ca^{2/3}$ at the midpoint of the polygonal channel in the limit of $Ca \to 0$ (Wong *et al.*, 1995), as was predicted previously (Bretherton, 1961). Also, the pressure drop (Δp) between the front and the back of the bubble was reported to be proportional to $Ca^{-1/3}$ (Wong *et al.*, 1995). Recently, Kreutzer *et al.* (2005) expanded Bretherton's correlation as $\Delta p \sim \frac{c_1}{Re}\left(1 + c_2\left(\frac{Re}{Ca}\right)^{0.33}\right)$ for bubble flows in circular channel in the range of $Re \sim O(100)$ and $Ca \sim O(0.01)$. For bubble flows in microchannel, Fuerstman *et al.* (2007) proposed a fully predictive model as a form of $\Delta p \sim c_1 + c_2 Ca^{-1/3}$. So far, however, the related works have been restricted only to the bubble flows, *i.e.*, for very small χ. Therefore, it will be meaningful to explore the droplet flows for non-negligible χ cases.

Droplet microfluidics is often utilized to investigate the pressure drop of the droplet flow as a methodology. Adzima and Velanka (2006) showed that an excess pressure drop was required for water-oil emulsions even if the viscosity of the droplet was smaller than that of the medium in the microchannel. Possible causes for the excess pressure drop are considered as an additional viscous stress induced by the velocity gradient near the droplet, a capillary pressure of the droplet, and the Marangoni stress due to the gradient of surfactant concentration on the interface (Olbricht, 1996). The contribution of the excess pressure drop induced by the droplet flow to the total pressure drop becomes significant as the channel size decreases (Chung and Kawaji, 2004). In microchannels, therefore, it is important to investigate the pressure drop and the pressure profiles near the droplet. For the complicated geometry, the pressure drop was also studied for droplet manipulation. In recent works (Chio *et al.*, 2006a; 2006b), the transient pressure drop was first measured when a bubble is passing through the circular microchannel with a smooth contraction. Chio *et al.* (2006a; 2006b) showed a good agreement with predictions of a theoretical model for quasi-stationary motion of a gas bubble (Jensen *et al.*, 2004) and their experimental works. In a contraction/expansion microchannel, Abkarian *et al.* (2006) showed that a stiffer red blood cell requires more pressure drop than a healthy one, which implies that a lower Ca droplet might induce additional pressure drop. In the present work, we focus on the pressure drop between the entrance and exit of the narrow channel with a finite element based front tracking method (Chung *et al.*, 2008). The objective of the present work is to investigate the pressure drop and the film thickness variation for various parameters set such as droplet size, fluid viscosity, Ca and fluid elasticity, and to propose an indirect relation between the pressure drop and the film thickness when the droplet is manipulated in the contraction - straight channel - expansion microchannel.

This paper is structured as follows. The governing equations, problem definition, flow geometry and computational meshes are presented in the next section. In Sec. 3, we present two scaling relations between the pressure drop and Ca, and the film thickness and Ca for various χ. We deduce a general conclusion that the pressure drop is strongly related with the film thickness by investigating the effects of droplet size, flow history of the droplets and fluid elasticity. In the final section, we propose relevant physics based on the observations on the droplet flows in microfluidics.

2. Numerical method

2.1. Governing equations

We consider isothermal, incompressible, creeping and immiscible two-phase fluid flow. The Oldroyd-B model is used as a constitutive equation for the viscoelastic fluid. Momentum, continuity and constitutive equations can be denoted as follows:

$$\nabla p - \eta_s \nabla \cdot (\nabla \mathbf{u} + (\nabla \mathbf{u})^T) - \nabla \cdot \boldsymbol{\tau} - \sigma \kappa \mathbf{n}_I \delta(\mathbf{x} - \mathbf{x}_p) = 0, \quad (1a)$$

$$\nabla \cdot \mathbf{u} = 0, \quad (1b)$$

$$\frac{\partial \mathbf{C}}{\partial t} + \mathbf{u} \cdot \nabla \mathbf{C} - (\nabla \mathbf{u})^T \cdot \mathbf{C} - \mathbf{C} \cdot \nabla \mathbf{u} = -\frac{1}{\lambda}(\mathbf{C} - \mathbf{I}), \quad (1c)$$

where p is the pressure, η_s the solvent viscosity, $\mathbf{u}$ the velocity vector, $\boldsymbol{\tau}$ the extra-stress tensor, σ the interface tension coefficient, κ twice the local mean curvature (total curvature) of the interface, $\mathbf{n}_I$ an outward unit normal vector from the interface, and $\delta(\mathbf{x} - \mathbf{x}_p)$ the Dirac delta function which is non-zero only at $\mathbf{x} = \mathbf{x}_p$. Here, $\mathbf{x}$ is the position vector in the domain and $\mathbf{x}_p$ is the position vector to designate the interface location. In the constitutive equation (1c), $\mathbf{C}$ is the conformation tensor, t the time, λ the relaxation time of the polymer and $\mathbf{I}$ the identity tensor, respectively. Superscript T means the transpose of a tensor. The relationship between the extra stress tensor $\boldsymbol{\tau}$ and the con-

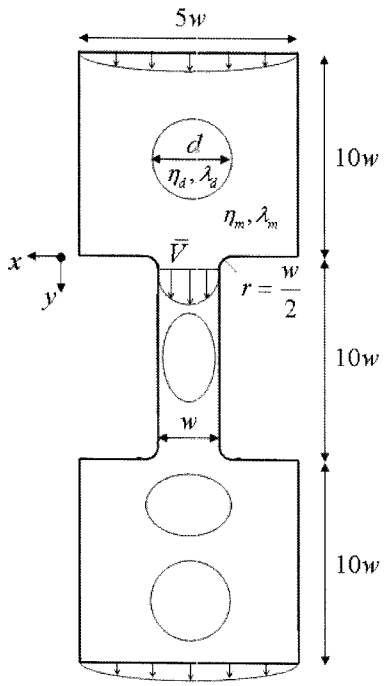

Fig. 1. Schematic diagram of the problem: a droplet passing through 5:1:5 contraction - straight channel - expansion flow.

formation tensor **C** is given by

$$\boldsymbol{\tau} = \frac{\eta_p}{\lambda}(\mathbf{C}-\mathbf{I}), \tag{2}$$

where η_p is the polymer viscosity. The relative solvent contribution to the solution viscosity η is defined as

$$\beta = \frac{\eta_s}{\eta_p + \eta_s} = \frac{\eta_s}{\eta}, \tag{3}$$

where η_s is the solvent viscosity. β is assumed to be 0.5 for viscoelastic fluids following the literatures (Chinyoka *et al.*, 2005; Chung *et al.*, 2008; Pillapakkam and Singh, 2001; Yue *et al.*, 2005).

Here, we use the previously developed FE-FTM algorithm (Chung *et al.*, 2008) to deal with the droplet dynamics in microchannel flow. We discretize the above equations (1a)-(1c) with finite element formulation. DEVSS-G (Liu *et al.*, 1998), SUPG (Brooks and Hughes, 1982) and matrix logarithm algorithms (Hulsen *et al.*, 2005) are applied to the governing equations to enhance numerical stability. For interface tracking and the calculation of interfacial tension, the front tracking method (Tryggvason *et al.*, 2001) is used. The readers who are interested in details can refer to our previous paper (Chung *et al.*, 2008).

2.2. Problem definition

The geometry used in this study is the same as our previous work (Chung *et al.*, 2008). Schematic diagram of the droplet dynamics in 5:1:5 planar contraction/expansion flow is shown in Fig. 1. The length of narrow channel is ten times the channel width w, the length of upstream and downstream channel is also $10w$. At the inlet and outlet, the fully-developed boundary condition is imposed for the velocity and the extra stress. The corners at the entrance and exit of the narrow channel are rounded with $r = w/2$ to

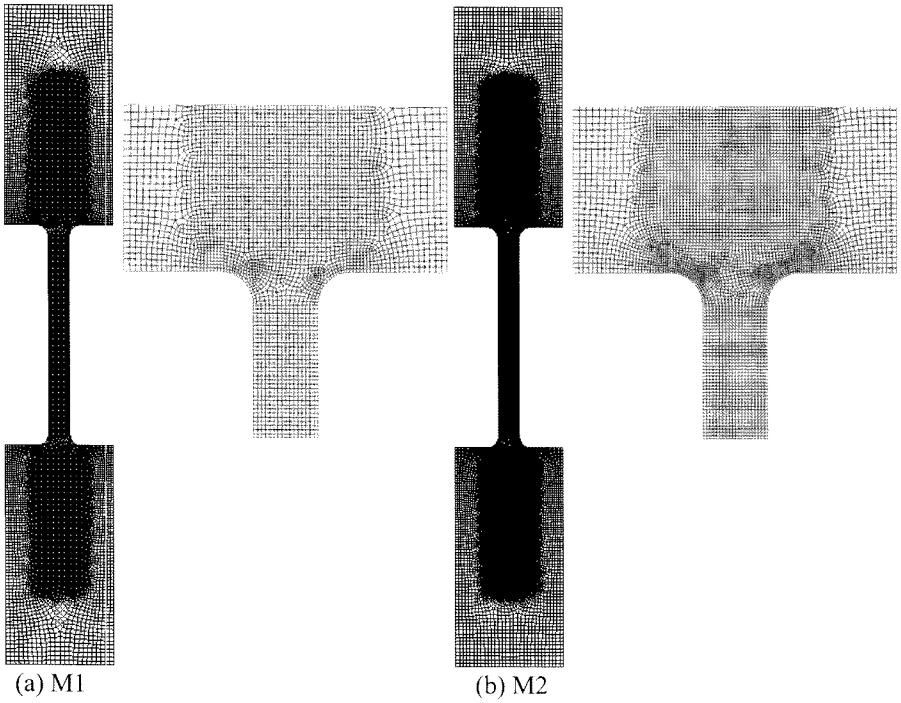

Fig. 2. Mesh configurations of whole domain and zoomed view of contraction region. (a) M1 and (b) M2.

Table 1. Detailed information of meshes used in this study

Name	Elements	Nodes	DOF	$\Delta x_{min}/w$
M1	16,561	67,045	369,952	0.0625
M2	25,010	101,005	533,419	0.05

help the droplet interface to flow smoothly and to avoid numerical singularity of the extra stress. The viscosity and relaxation time of the fluids are designated as η_i and λ_i, where the subscript i represents droplet (d) or medium (m). At the initial state, a single droplet with diameter d is positioned $5w$ upward from the entrance of the narrow channel, and passes through the contraction and expansion geometry.

In this problem, three important dimensionless numbers are considered: viscosity ratio between droplet and medium (χ), capillary number (Ca) and Deborah number (De_i) of fluid i, which are defined as follows:

$$\chi = \frac{\eta_d}{\eta_m}, \tag{4}$$

$$Ca = \frac{\eta_m \bar{V}}{\sigma}, \tag{5}$$

$$De_i = \frac{\lambda_i \bar{V}}{w/2}, \tag{6}$$

where $\bar{V}$ is the mean velocity in the narrow channel. De_i represents two cases, *i.e.*, De_d is defined for a viscoelastic droplet in Newtonian medium (VN) and De_m is for a Newtonian droplet in viscoelastic medium (NV). β_i is also defined for viscoelastic fluids in the same way.

We prepare two meshes: M1 and M2. Mesh configurations are shown in Fig. 2 with a zoomed view near the contraction. M2 mesh is the same one used in our previous study (Chung *et al.*, 2008). All results given in the current study are based on M2, and M1 is used for mesh refinement test only. More details on meshes used in the study are given in Table 1.

3. Results and discussion

3.1. Pressure drop in Newtonian droplet/Newtonian medium

3.1.1. Excess pressure drop

The prediction of the pressure drop for the flow through the microchannel containing a droplet is more complicated than a single phase flow problem. For comparison purpose, we measure the pressure profile along the centerline from the inlet to the outlet in the whole domain for a single phase flow as shown in Fig. 3(a), which shows a decreasing pressure profile in the narrow channel ($0<y<10$). The pressure is non-dimensionalized with the characteristic wall shear stress, $\frac{\eta_m \bar{V}}{w/2}$.

When the droplet passes through the narrow channel, the pressure drop (Δp) shows a fluctuation at the entrance and at the exit region, respectively, as shown in Fig. 3(b). In the previous numerical (Queguiner and Barthes-Biesel, 1997) and experimental study (Secomb and Hsu, 1995) using a red blood cell, a similar fluctuation of the pressure drop

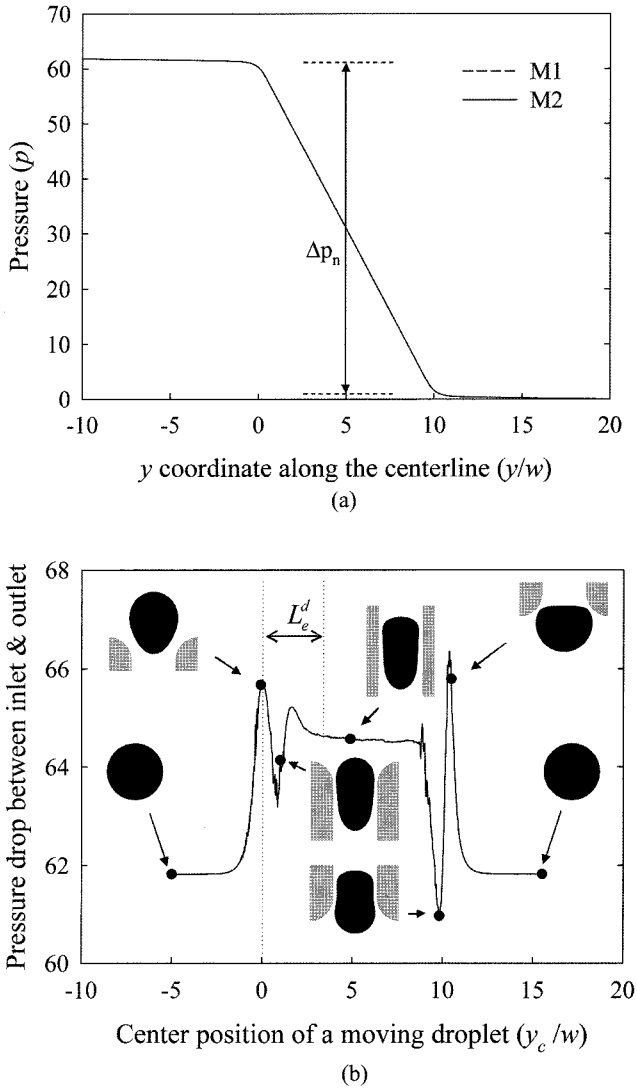

Fig. 3. Pressure profiles in the 5:1:5 contraction - straight channel - expansion flow. (a) Pressure along the centerline for single phase flow. (b) Transient pressure drop between inlet and outlet of the computational domain with a droplet (M2, χ=1, d=50, Ca=0.1).

was predicted in the cylindrical contraction/expansion flow. Queguiner and Barthes-Biesel (1997) argued that the fluctuation is related with the capsule motion for a short time and the viscoelastic process of the membrane. We also attribute the fluctuation in Fig. 3(b) to the complicated droplet deformation process at the entrance and the exit.

If we define the entry length (L_e^d) as a moving distance of the droplet until the pressure becomes constant in the narrow channel as shown in Fig. 3(b), we obtain an approximate value of $\frac{L_e^d}{w/2} \sim 2.55$ for equiviscous droplet of $d=50$ and $Ca=0.1$, whereas the entry length for the planar laminar flow (L_e) of a single phase is predicted as $\frac{L_e}{w/2} \rightarrow 0$ as $Re \rightarrow 0$ (Denn, 1980), where Re is the Reynolds number characterized with the mean velocity in the channel. Since the creeping flow is considered in the current study, we expect that L_e approaches zero for a single phase flow, *i.e.*, the slope of pressure versus y-coordinate is changed abruptly at the entrance region as shown in Fig. 3(a). For the droplet flow, L_e^d is expected to approach the droplet size in the limit case since a fluctuation of the pressure is observed in the entrance region in Fig. 3(b). In other words, L_e^d is expected to decrease with decreasing Ca since low Ca means relatively strong interface tension compared to the viscous stress of the fluid.

Although the pressure drop (Δp) shows fluctuations at the entrance ($y/w=0$) and at the exit region ($y/w=10$) according to the droplet motion, we observe the plateau region of pressure drop in the narrow channel as shown in Fig. 3(b). In the present study, we mainly focus on the steady pressure drop when the droplet passes the narrow channel. In case of $\chi=1$ and $Ca=0.1$, the steady pressure drop is relatively larger than the pressure drop for a single phase flow. In order to quantify the difference in the pressure drop against the single phase flow, we define an excess pressure drop (Δp^+) between entrance and exit of the narrow channel as follows (Adzima and Velankar, 2006):

$$\Delta p^+ = \Delta p_2 - \Delta p_1 , \tag{7}$$

where Δp_2 is the steady pressure drop between entrance and exit of the droplet flow, and Δp_1 is the steady pressure drop for a single phase flow. We notice that Δp_n is defined as a pressure drop between the entrance ($y/w=0$) and exit ($y/w=10$) of the narrow channel as shown in Fig. 3(a), not between inlet ($y/w=-10$) and outlet ($y/w=20$). In the following section, we investigate the effect of droplet size, Ca and fluid elasticity on the excess pressure drop (Δp^+). We expect that Δp^+ is strongly dependent on droplet size, χ, Ca, and De.

3.1.2. Effect of droplet size and *Ca*

We begin with equiviscous case ($\chi=1$) with changing

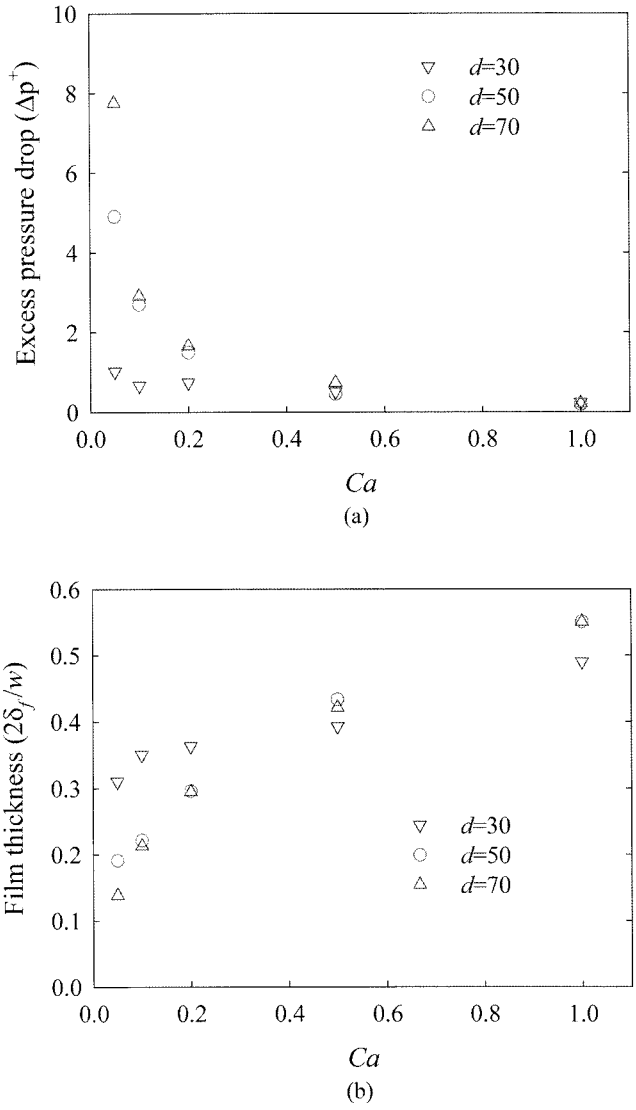

Fig. 4. Effect of droplet size on (a) the excess pressure drop and (b) the film thickness with increasing Ca (M2, $\chi=1$).

droplet size and Ca. Fig. 4(a) clearly shows that Δp^+ depends on the droplet size and Ca, and the dependency on Ca is more relevant for larger droplets ($d=50$, 70) compared with smaller case ($d=30$). Note that the latter ($d=30$) is smaller than the channel width ($w=40$). Thus, the blockage by the droplet is not severe compared with lager droplets, which results in smaller Δp^+. The present observation is similar to the previous experimental work on water-oil emulsions (Adzima and Velankar, 2006) such that the excess pressure may be neglected if the droplets are smaller than the cross-sectional dimension of the microchannel. This implies that the excess pressure drop (Δp^+) is strongly related with a film thickness (δ_f) between the droplet interface and the channel wall. In this study, the film thickness is measured at the mid-point of the droplet as depicted in Fig. 5(a).

For larger droplets, Δp^+ increases sharply with decreasing

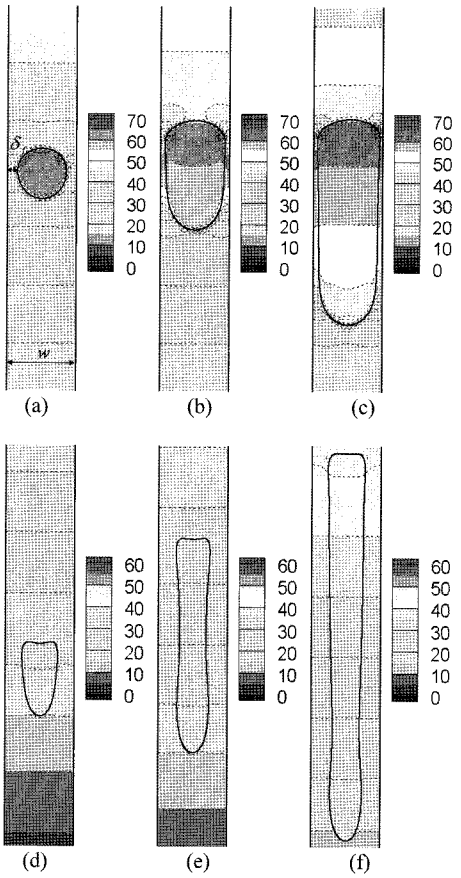

Fig. 5. Pressure contours near the droplet confined in the narrow channel (M2, χ=1). (a) d=30, Ca=0.05. (b) d=50, Ca=0.05. (c) d=70, Ca=0.05. (d) d=30, Ca=1. (e) d=50, Ca=1. (f) d=70, Ca=1.

Ca since the blockage effect of the droplet becomes significant as Ca decreases, *i.e.*, the film thickness (δ_f) decreases as Ca decreases as shown in Fig. 4(b). In Fig. 5, we present pressure contours near the droplet for low Ca (Figs. 5.(a)-(c)) and for large Ca (Figs. 5(d)-(f)). In Figs. 5(b)-(c), large droplets of low Ca look like fitting pistons in the narrow channel. Therefore, we conclude that the enhancement of the excess pressure drop as $Ca \rightarrow 0$ is attributed to the blockage effect of the droplet in the narrow channel. In addition, we conjecture that the droplets with low Ca show development of high pressure inside the droplet in order to sustain the droplet shape against relatively strong interfacial tension as shown in Figs. 5(a)-(c). On the contrary, in case of large Ca as shown in Figs. 5(d)-(f), lower pressure is developed inside the droplet since large Ca means relatively weak interfacial tension to viscous stress.

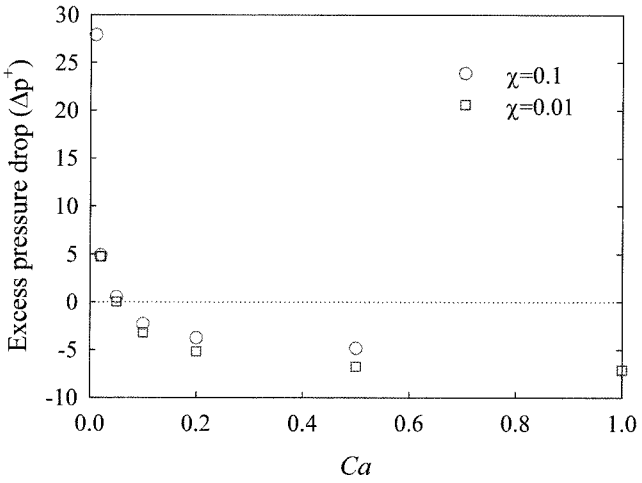

Fig. 6. Excess pressure drop (Δp^+) of droplets less viscous than medium with increasing Ca (M2, d=50).

3.1.3. Effect of viscosity ratio (χ)

In this section, we consider the droplet of d=50. For droplets less viscous than medium such as χ=0.1 and 0.01, the dependency of Δp^+ on δ_f is also observed. Fig. 6 shows that Δp^+ is inversely proportional to Ca as in Fig. 4(a). In Fig. 7, we present the film thickness and the pressure con-

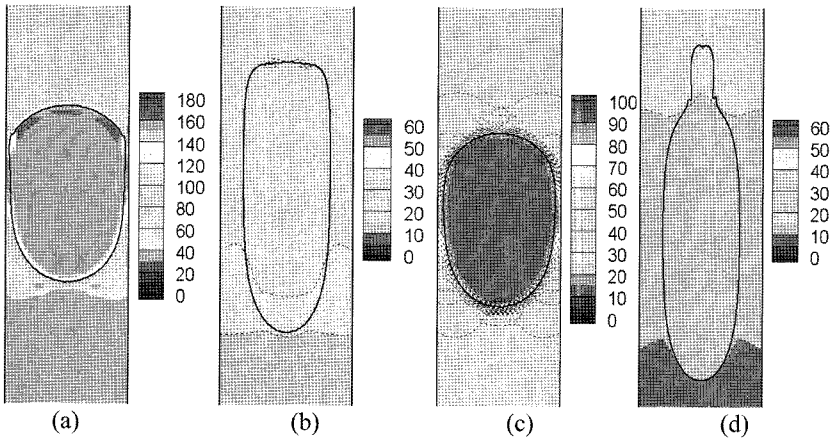

Fig. 7. Pressure contours near the droplets confined in the narrow channel (M2, d=50). (a) χ=0.1, Ca=0.01, $2\delta_f/w$=0.07. (b) χ=0.1, Ca=0.5, $2\delta_f/w$=0.34. (c) χ=0.01, Ca=0.02, $2\delta_f/w$=0.09. (d) χ=0.01, Ca=1, $2\delta_f/w$=0.37.

tour near the droplet for relevant cases. We clearly observe that the film thickness decreases as Ca decreases. As shown in Figs. 7(c) and (d), the pressure contour is nearly uniform inside the droplet for small χ, which assists the assumption of Fuerstman *et al.* (Fuerstman *et al.*, 2007). They assumed that the pressure is uniform inside the bubble in liquid emulsion system ($\chi \sim 0.001$). However, we observe that the pressure distribution is not any more uniform for $\chi \geq 0.1$ as shown in Figs. 5 and 7(a)-(b).

It is worthwhile to note that there is a positive excess pressure drop for small Ca although less viscous droplets are manipulated. In Fig. 6, we observe that the sign of Δp^+ is changed for $\chi=0.1$ and 0.01 depending on Ca, *i.e.*, the positive Δp^+ is predicted for $Ca \leq 0.05$. The positive excess pressure drop was also reported for water-oil emulsions ($\chi \sim 1/2.95$) in microchannel (Adzima and Velankar, 2006). In droplet-related experiments, Ca typically ranges in between $10^{-3} \sim 10^{1}$ in microchannel flow (Christopher and Anna, 2007), thus, we expect that the excess pressure drop can be positive at lower Ca independent of χ in most cases for droplet microfluidics.

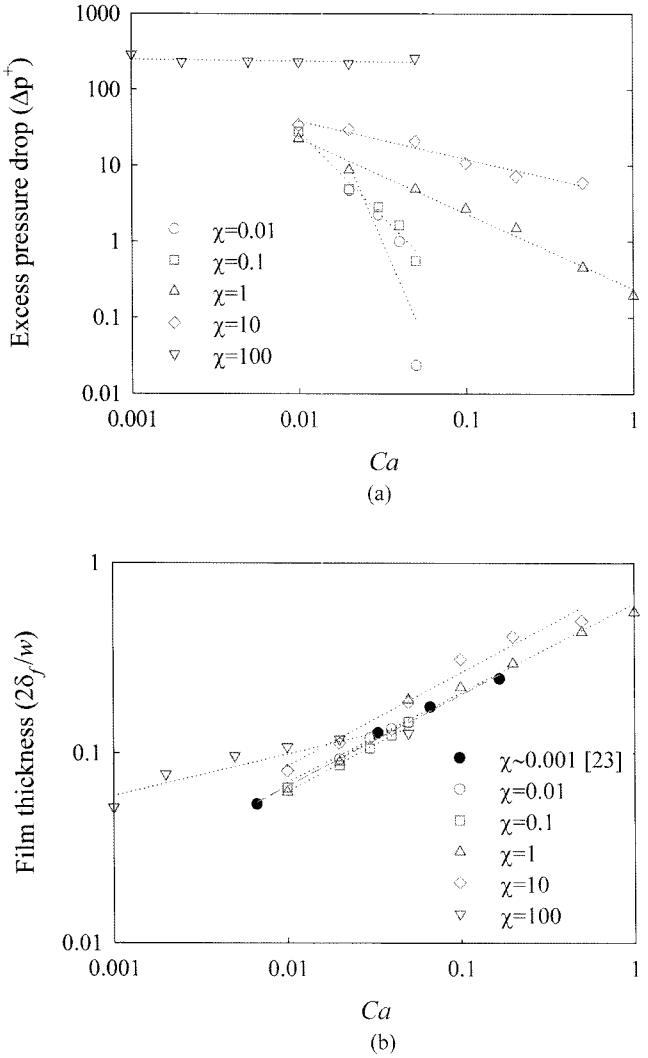

Fig. 8. Scaling behavior for various viscosity ratio (χ). (a) The excess pressure drop (Δp^+) - Ca. (b) The film thickness ($2\delta_f/w$) - Ca.

To investigate the relationship between Δp^+ and Ca, we present Δp^+-Ca graph for various χ in Fig. 8(a). We choose the range of Ca such that the positive excess pressure drop is predicted. In the figure, a scaling relationship of $\Delta p^+ \sim Ca^m$ can be found. It is observed that m is negative irrespective of χ, which implies that Δp^+ increases with decreasing Ca independent of χ. The dependency on Ca becomes strong with decreasing χ since the slope (m) decreases with decreasing χ.

Also, we note that the level of excess pressure drop generally increases with increasing χ. For instance, the excess pressure drop (Δp^+) for the droplet of $\chi=100$ is much enhanced compared with Δp_1 (*cf.* $\Delta p_1=58.59$), which is reasonable since $\Delta p \propto \eta$ for the laminar flow (Morris and Forster, 2004). For highly viscous droplet such as $\chi=100$, a dominant factor on large Δp^+ is considered to be the enhanced viscous stress due to large χ. For the same reason, the level of Δp^+ of $\chi=10$ is lower than that for $\chi=100$. Consequently, it is observed that the excess pressure drop (Δp^+) is roughly proportional to χ for $\chi \geq 1$.

In Fig. 8(b), we observe another scaling behavior for the film thickness as $\delta_f \sim Ca^n$. In table 2, we present fitted parameters for the excess pressure drop and for the film thickness. We find that n is positive for all χ, which simply means that δ_f decreases with decreasing Ca. Here, we note that the current work presents the power-law relationship for the excess pressure drop and for the film thickness depending on the viscosity ratio (χ), which is missing in the previous works (Bretherton, 1961; Fuerstman *et al.*, 2007; Wong *et al.*, 1995; 1995). We compare our results with the previous work (Heil, 2001) for two-dimensional bubbles between parallel plates. We get a good agreement between our data ($\delta_f \sim Ca^{0.49}$) for $\chi=0.01$ and Heil's result (Heil, 2001) ($\delta_f \sim Ca^{0.48}$) for creeping bubble flows of $\chi \sim 0.001$ as shown in Fig. 8(b). Note that Heil's result in Fig. 8(b) was reproduced from the data at $Re=0$ in his Fig. 2 (Heil, 2001). We observe that the exponent n is nearly close to 0.5 in the Ca range of $O(10^{-2}) \sim O(1)$ except data

Table 2. Power-law parameters as $\Delta p^+ \sim Ca^m$ and $\delta_f \sim Ca^n$ at each χ

χ	m	n
0.01	–5.13	0.49
0.1	–2.25	0.49
1	–0.99	0.47
10	–0.50	0.49
100	–0.02	0.22

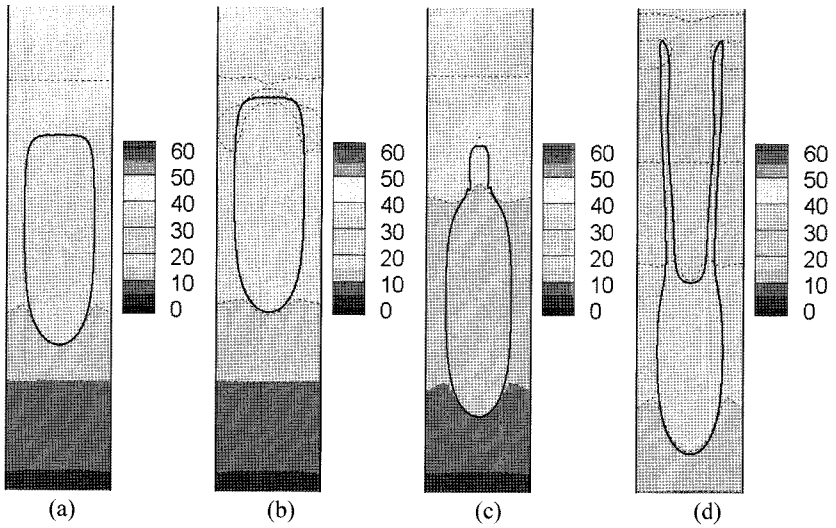

Fig. 9. Effect of flow history of the droplet on the pressure contours and droplet deformation in the narrow channel (M2, d=50, χ=0.01). (a) Initialized at wide channel, Ca=0.5. (b) Initialized at narrow channel, Ca=0.5. (c) Initialized at wide channel, Ca=1. (d) Initialized at narrow channel, Ca=1.

for χ=100 in Table 2. As discussed earlier, for highly viscous droplet such as χ=100, the variation in Δp^+ due to Ca change becomes insignificant.

3.1.4. Effect of flow history

In this section, we will check the assumption that the excess pressure drop is strongly affected by the film thickness. We initialize the droplet at different positions, *i.e.*, at the wide channel ($y_c/w=-5$) as usual, and at the entrance region in the narrow channel ($y_c/w\sim0.12$). As shown in Figs. 9(a) and (b), there is no difference on the droplet deformation and pressure contours for small Ca. However, an obvious difference is observed for large Ca as shown in Figs. 9(c) and (d). Therefore, we conclude that a tadpole-like shape shown in Fig. 9(c) is attributed to the history of contraction flow at the entrance region.

On the other hand, we observe that the excess pressure drop (Δp^+) is nearly unchanged although the different shape of the droplet is observed in Figs. 9(c) and (d). For instance, Fig. 9(d) shows only 1.3% of increase in Δp^+ with respect to that of Fig. 9(c). This can be attributed to the similar film thickness in both cases ($2\delta_f/w$=0.373, 0.382 in Figs. 9(c) and (d), respectively). Although the viscous stress and capillary stress are different due to the difference in the droplet shape, we observe no drastic change of the excess pressure drop. Therefore, we conclude that the film thickness is one of the dominant factors on the excess pressure drop over the flow history.

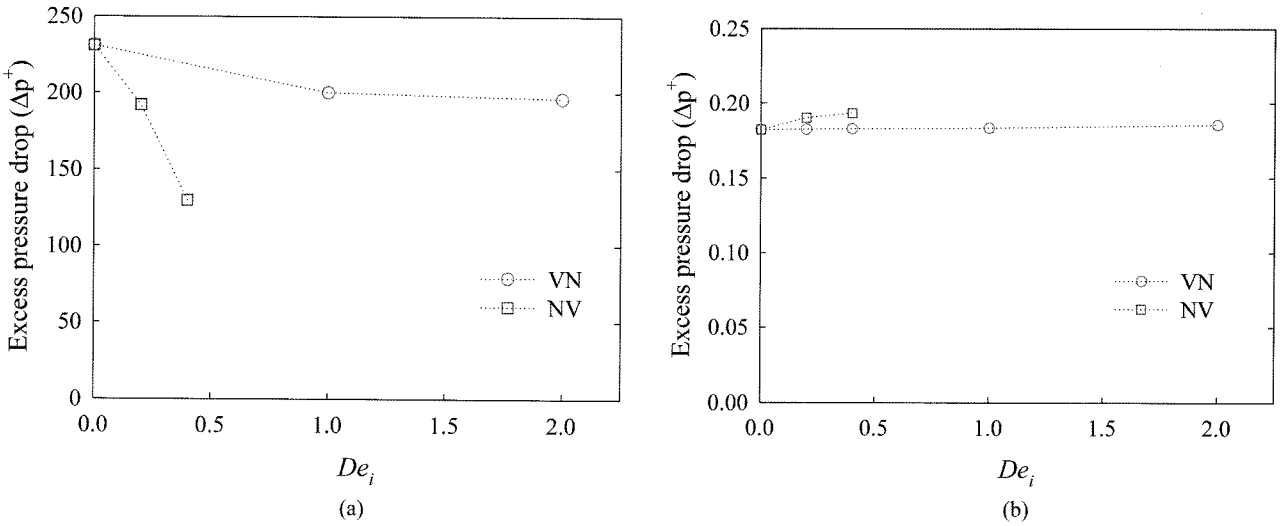

Fig. 10. Effect of fluid elasticity on the excess pressure drop (Δp^+) with increasing De_i (M2, d=50). (a) χ=100, Ca=0.01. (b) χ=10, Ca=0.1.

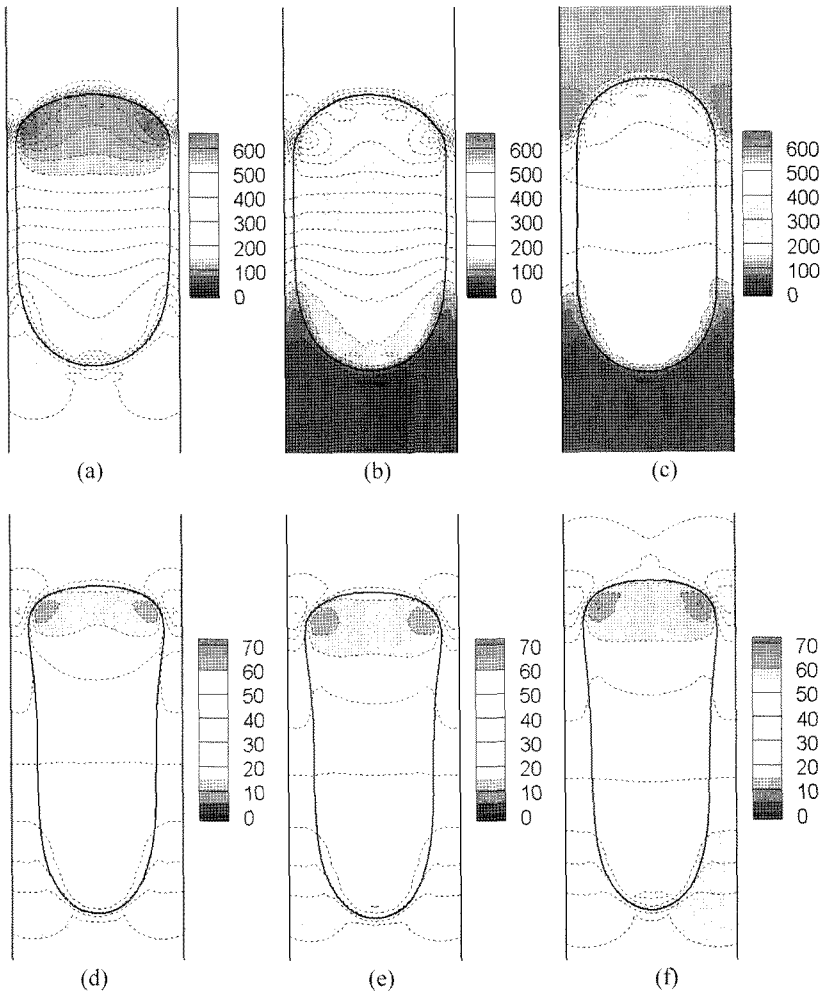

Fig. 11. Effect of fluid elasticity on pressure contours near the droplets more viscous than medium confined in the narrow channel (M2, d=50). χ=100, Ca=0.01 for (a)-(c), and χ=10, Ca=0.1 for (d)-(f). (a) NN, $2\delta_f/w$=0.111. (b) VN, De_d=2,$2\delta_f/w$=0.115. (c) NV, De_m=0.4, $2\delta_f/w$=0.186. (d) NN, $2\delta_f/w$=0.310. (e) VN, De_d=2,$2\delta_f/w$=0.301. (f) NV, De_m=0.4, $2\delta_f/w$=0.306.

3.2. Effect of fluid elasticity

Here we investigate the effect of fluid elasticity on the excess pressure drop using the Oldroyd-B model. We observe that the effect of fluid elasticity on Δp^+ is relevant only at χ=100, whereas the effect was negligible for other χ values, which will be discussed later. For χ=100, Fig. 10(a) shows that Δp^+ decreases sharply when the Newtonian droplet flows in the viscoelastic medium (NV), whereas Δp^+ is nearly unchanged when the viscoelastic droplet is manipulated in the Newtonian medium (VN). The difference between NV and VN cases originates from the difference in the film thickness. NV case shows the largest film thickness of $2\delta_f/w$=0.186 as in Fig. 11(c). In our previous study (Chung *et al.*, 2008), we attributed the development of the thick film to the high normal stress development in the viscoelastic film region. Therefore, the enhancement of the film thickness due to the normal stress development results in the sharp reduction of Δp^+ as De_m increases as shown in Fig. 10(a).

In the meanwhile, we observe no significant difference in the excess pressure drop with increasing De_i for both VN and NV cases at χ=10 as in Fig. 10(b), which can be attributed to the similar film thickness irrespective of the difference in viscoelasticity. As shown in Figs. 11(d)-(f), the fluid elasticity does not significantly affect Δp^+ and pressure contour near the droplet compared with NN case (Fig. 11(d)).

4. Concluding remarks

We investigated the excess pressure drop (Δp^+) when the droplet is manipulated in the contraction - straight channel - expansion type microchannel. First, the excess pressure drop was found to be strongly dependent on the viscosity ratio (χ), *i.e.*, the level of the excess pressure drop increases as χ increases, which is reasonable since larger pressure drop is required to flow more viscous fluids. We predict positive Δp^+ as Ca decreases even when the less

viscous droplet is manipulated than the medium. The excess pressure drop seems inversely proportional to Ca for all χ considered in the present work, which implies that Δp^+ is strongly related with the droplet blockage effect or the film thickness since the film thickness (δ_f) is a growth function of Ca. Finally, we observed scaling relations as $\Delta p^+ \sim Ca^m$ and $\delta_f \sim Ca^n$ when manipulating relatively short droplets comparable to the channel width. We found that the exponent m decreases as χ decreases for nearly-packed droplets, and that the exponent n is close to 0.5 for $\chi \leq 10$ in the Ca range of $O(10^{-2}) \sim O(1)$. These simple relations would be helpful for understanding droplet flows and for expecting the pressure drop in designing the experiments in microfluidics.

We also observed a clue for the strong relation between the excess pressure drop and the droplet blockage (or the film thickness) in the narrow channel. First, for $\chi \leq 10$, a decrease in the film thickness results in an increase of the excess pressure drop as Ca decreases. Second, the excess pressure drop is nearly similar only if the film thickness is similar although the capillary stress and the viscous stress are differently developed due to the different flow history. Third, as for the effect of fluid elasticity, the sharp reduction of the excess pressure drop as De_m increases in NV case is attributed to the increase of the film thickness due to the normal stress development in the film region. Therefore, we conclude that the blockage effect of the droplet (decrease in the film thickness) in the narrow channel plays a significant role in enhancing the excess pressure drop.

We hope that this study would be helpful in understanding underlying physics in the droplet channel flow and in designing the related experiments for various applications in droplet microfluidics.

Acknowledgements

The authors wish to acknowledge the National Research Laboratory Fund (M10300000159) of the Ministry of Science and Technology in Korea. The authors would like to acknowledge the support from KISTI Supercomputing Center (KSC-2007-S00-3004).

References

Abkarian, M., M. Faivre and H. A. Stone, 2006, High-speed microfluidic differential manometer for cellular-scale hydrodynamics, *PNAS* **103(3)**, 538-542.

Abraham, S., E. H. Jeong, T. Arakawa, S. Shoji, K. C. Kim, I. Kim and J. S. Go, 2006, Microfluidics assisted synthesis of well-defined spherical polymeric microcapsules and their utilization as potential encapsulants, *Lab Chip* **6(6)**, 752-756.

Adzima, B. J. and S. S. Velankar, 2006, Pressure drops for droplet flows in microfluidic channels, *J. Micromech. Microeng.* **16(8)**, 1504-1510.

Bretherton, F. P., 1961, The motion of long bubbles in tubes, *J. Fluid Mech.* **10**, 166-188.

Bringer, M. R., C. J. Gerdts, H. Song, J. D. Tice and R. F. Ismagilov, 2004, Microfluidic systems for chemical kinetics that rely on chaotic mixing in droplets, *Philos. T. Roy. Soc. A* **362 (1818)**, 1087-1104.

Brooks, A. N. and T. J. R. Hughes, 1982, Streamline upwind Petrov-Galerkin formulations for convection dominated flows with particular emphasis on the incompressible Navier-Stokes equations, *Comput. Method Appl. Mech. Engrg.* **32(1-3)**, 199-259.

Chinyoka, T., Y. Y. Renardy, A. Renardy and D. B. Khismatullin, 2005, Two-dimensional study of drop deformation under simple shear for Oldroyd-B liquids, *J. Non-Newtonian Fluid Mech.* **130(1)**, 45-56.

Chio, H., M. J. Jensen, X. L. Wang, H. Bruus and D. Attinger, 2006a, On the motion of a bubble through microchannel contractions, *NSTI-Nanotech.* **2**, 497-500.

Chio, H., M. J. Jensen, X. L. Wang, H. Bruus and D. Attinger, 2006b, Transient pressure drops of gas bubbles passing through liquid-filled microchannel contractions: an experimental study, *J. Micromech. Microeng.* **16(1)**, 143-149.

Christopher, G. F. and S. L. Anna, 2007, Microfluidic methods for generating continuous droplet streams, *J. Phys. D: Appl. Phys.* **40(19)**, R319-R336.

Chu, L. Y., A. S. Utada, R. K. Shah, J. W. Kim and D. A. Weitz, 2007, Controllable monodisperse multiple emulsions, *Angew. Chem. Int. Edit.* **46(47)**, 8970-8974.

Chung, C., M. A. Hulsen, J. M. Kim, K. H. Ahn and S. J. Lee, 2008, Numerical study on the effect of viscoelasticity on drop deformation in simple shear and 5:1:5 planar contraction/expansion microchannel, *J. Non-Newtonian Fluid Mech.* **155**, 80-93.

Chung, P. M. Y. and M. Kawaji, 2004, The effect of channel diameter on adiabatic two-phase flow characteristics in microchannels, *Int. J. Multiphase Flow* **30(7-8)**, 735-761.

Cox, B. G., 1962, On driving viscous fluid out of a tube, *J. Fluid Mech.* **14**, 81-96.

Denn, M. M., 1980, Process fluid mechanics, Prentice-Hall, Inc.

Edvinsson, R. K. and S. Irandoust, 1996, Finite-element analysis of Taylor flow, *AIChE J.* **42(7)**, 1815-1823.

Fairbrother, F. and A. E. Stubbs, 1935, Studies in electroendosmosis. Part VI. The bubble-tube method of measurements, *J. Chem. Soc.* **1**, 527-529.

Fuerstman, M. J., A. Lai, M. E. Thurlow, S. S. Shevkoplyas, H. A. Stone and G. M. Whitesides, 2007, The pressure drop along rectangular microchannels containing bubbles, *Lab Chip* **7(11)**, 1479-1489.

Giavedoni, M. D. and F. A. Saita, 1997, The axisymmetric and plane cases of a gas phase steadily displacing a Newtonian liquid - A simultaneous solution of the governing equations, *Phys. Fluids* **9(8)**, 2420-2428.

Giavedoni, M. D. and F. A. Saita, 1999, The rear meniscus of a long bubble steadily displacing a Newtonian liquid in a capillary tube, *Phys. Fluids* **11(4)**, 786-794.

Griffiths, A. D. and D. S. Tawfik, 2003, Directed evolution of an extremely fast phosphotriesterase by in vitro compartmental-

ization, *EMBO J.* **22(1)**, 24-35.

He, M. Y., J. S. Edgar, G. D. M. Jeffries, R. M. Lorenz, J. P. Shelby and D. T. Chiu, 2005, Selective encapsulation of single cells and subcellular organelles into picoliter- and femtoliter-volume droplets, *Anal. Chem.* **77(6)**, 1539-1544.

Heil, M., 2001, Finite Reynolds number effects in the Bretherton problem, *Phys. Fluids* **13(9)**, 2517-2521.

Hulsen, M. A., R. Fattal and R. Kupferman, 2005, Flow of viscoelastic fluids past a cylinder at high Weissenberg number: stabilized simulations using matrix logarithms, *J. Non-Newtonian Fluid Mech.* **127(1)**, 27-39.

Jensen, M. J., G. Goranovic and H. Bruus, 2004, The clogging pressure of bubbles in hydrophilic microchannel contractions, *J. Micromech. Microeng.* **14(7)**, 876-883.

Kline, T. R., M. K. Runyon, M. Pothiawala and R. F. Ismagilov, 2008, ABO, D blood typing and subtyping using plug-based microfluidics, *Anal. Chem.* **80(16)**, 6190-6197.

Kreutzer, M. T., F. Kapteijn, J. A. Moulijn, C. R. Kleijn and J. J. Heiszwolf, 2005, Inertial and interfacial effects on pressure drop of Taylor flow in capillaries, *AIChE J.* **51(9)**, 2428-2440.

Laser, D. J. and J. G. Santiago, 2004, A review of micropumps, *J. Micromech. Microeng.* **14(6)**, R35-R64.

Liu, A. W., D. E. Bornside, R. C. Armstrong and R. A. Brown, 1998, Viscoelastic flow of polymer solutions around a periodic, linear array of cylinders: comparisons of predictions for microstructure and flow fields, *J. Non-Newtonian Fluid Mech.* **77(3)**, 153-190.

Morris, C. J. and F. K. Forster, 2004, Oscillatory flow in microchannels: comparison of exact and approximate impedance models with experiments, *Exp. Fluids* **36(6)**, 928-937.

Olbricht, W. L., 1996, Pore-scale prototypes of multiphase flow in porous media, *Ann. Rev. Fluid Mech.* **28**, 187-213.

Pillapakkam, S. B. and P. Singh, 2001, A level-set method for computing solutions to viscoelastic two-phase flow, *J. Comput. Phys.* **174(2)**, 552-578.

Queguiner, C. and D. Barthes-Biesel, 1997, Axisymmetric motion of capsules through cylindrical channels, *J. Fluid Mech.* **348**, 349-376.

Ratulowski, J. and H. C. Chang, 1989, Transport of gas bubbles in capillaries, *Phys. Fluids A* **1(10)**, 1642-1655.

Reinelt, D. A., 1987, The rate at which a long bubble rises in a vertical tube, *J. Fluid Mech.* **175**, 557-565.

Secomb, T. W. and R. Hsu, 1995, Red blood cell mechanics and functional capillary density, *Int. J. Microcirc.* **15(5)**, 250-254.

Sepp, A., F. Ghadessy and Y. Choo, 2007, Cell-free selection of DNA-binding proteins for future gene therapy applications, *Gene Therapy and Regulation* **3(1)**, 51-63.

Shen, E. I. and K. S. Udell, 1985, A finite element study of low Reynolds number two-phase flow in cylindrical tubes, *J. Appl. Mech. Trans. ASME* **52(2)**, 253-256.

Song, H., J. D. Tice and R. F. Ismagilov, 2003, A microfluidic system for controlling reaction networks in time, *Angew. Chem. Int. Edit.* **42(7)**, 768-772.

Tawfik, D. S. and A. D. Griffiths, 1998, Man-made cell-like compartments for molecular evolution, *Nat. Biotechnol.* **16(7)**, 652-656.

Taylor, G. I., 1961, Deposition of a viscous fluid on the wall of a tube, *J. Fluid Mech.* **10**, 161-165.

Tryggvason, G., B. Bunner, A. Esmaeeli, D. Juric, N. Al-Rawahi, W. Tauber, J. Han, S. Nas and Y. J. Jan, 2001, A front-tracking method for the computations of multiphase flow, *J. Comput. Phys.* **169(2)**, 708-759.

Wong, H., C. J. Radke and S. Morris, 1995, The motion of long bubbles in polygonal capillaries.1. thin-films, *J. Fluid Mech.* **292**, 71-94.

Wong, H., C. J. Radke and S. Morris, 1995, The motion of long bubbles in polygonal capillaries. 2. drag, fluid pressure and fluid flow, *J. Fluid Mech.* **292**, 95-110.

Yue, P. T., J. J. Feng, C. Liu and J. Shen, 2005, Viscoelastic effects on drop deformation in steady shear, *J. Fluid Mech.* **540**, 427-437.

Zheng, B., J. D. Tice and R. F. Ismagilov, 2004, Formation of arrayed droplets of soft lithography and two-phase fluid flow, and application in protein crystallization, *Adv. Mater.* **16(15)**, 1365-1368.